Development 133, 4933-4944 (2006) doi:10.1242/dev.02679

Heparan sulfate biosynthetic gene *Ndst1* is required for FGF signaling in early lens development

Yi Pan[1], Andrea Woodbury[1], Jeffrey D. Esko[2], Kay Grobe[3] and Xin Zhang[1,*]

Multiple signaling molecules, including bone morphogenic proteins (BMP) and fibroblast growth factors (FGF), play important roles in early lens development. However, how these morphogens are regulated is still largely unknown. Heparan sulfate participates in both morphogen transport and morphogen-receptor interaction. In this study, we demonstrate that inactivation of the heparan sulfate biosynthetic gene *Ndst1* resulted in invagination defects of the early lens and in the disruption of lens-determination gene expression, leading to severe lens hypoplasia or anophthalmia. *Ndst1* mutants exhibited reduced sulfation of heparan sulfate, but both BMP- and Wnt-signaling remained unchanged. Instead, these embryos showed diminished binding of a subset of FGF proteins to FGF receptors. Consistent with disruption of FGF signaling, expression of phospho-Erk and *ERM* were also downregulated in *Ndst1*-mutant lenses. Taken together, these results establish an important role of *Ndst1* function in FGF signaling during lens development.

KEY WORDS: Ndst, HSPG, BMP, Wnt, FGF, Erk, Signaling, Lens, Induction, Mouse

INTRODUCTION

Multiple signaling pathways are involved in early-lens morphogenesis, including bone morphogenic proteins (BMPs), fibroblast growth factors (FGFs), Wnts and hedgehog (Hh). Genetic inactivation of *Bmp4* or *Bmp7* in mice abolished *Sox2* expression in the head ectoderm and disrupted lens-placode formation (Furuta and Hogan, 1998; Wawersik et al., 1999). Similarly, suppression of FGF signaling via a pharmacological inhibitor or dominant-negative FGF receptor 1 (FGFR1) resulted in the downregulation of *Pax6*, *Sox2* and *Foxe3* expression, and in defects in lens formation (Faber et al., 2001). In further support of a role of FGF signaling in early lens development, a mutation in the FGFR signaling mediator *Frs2α* led to anophthalmia or microphthalmia (Gotoh et al., 2004). Hh signaling is necessary for early eye-field specification and lens regeneration (Macdonald et al., 1995; Tsonis et al., 2004). However, hyperactive Hh signaling from the embryonic midline may also result in lens degeneration, as demonstrated in cavefish development (Yamamoto et al., 2004). Wnt signaling is also known to be involved in the development of the lens. Misexpression of a Wnt receptor, *frizzled 3*, led to ectopic *Pax6* expression and eye formation in *Xenopus* (Rasmussen et al., 2001). By contrast, a mouse mutant deficient for the Wnt signaling co-receptor *Lrp6* exhibited abnormal cell death in lens epithelium, whereas the conditional knockout of β-catenin in periocular ectoderm resulted in ectopic lentoid formation (Smith et al., 2005; Stump et al., 2003).

Many of the signaling pathways described above are known to be dependent on the presence of heparan sulfate proteoglycans (HSPGs) on the cell surface (reviewed in Lin, 2004). HSPGs are glycoproteins containing covalently linked heparan sulfate glycosaminoglycan chains. These linear polysaccharides exhibit enormous structural heterogeneity because of variable *N*-deacetylation of *N*-acetylglucosamine residues, N- and O-sulfation, and epimerization of uronic acid residues (Esko and Selleck, 2002). Previous studies have demonstrated that cell-surface proteoglycans can serve as co-receptors for FGF (Rapraeger et al., 1991; Yayon et al., 1991). This is supported by crystallographic structures of heparan sulfate associated with an FGF-FGFR complex (Pellegrini et al., 2000; Schlessinger et al., 2000). Recently, the role of HSPGs in morphogen diffusion was illuminated by genetic studies of *Drosophila* proteoglycan core proteins and glycosaminoglycan biosynthetic enzymes. It was demonstrated that loss of HSPGs prevented the transport of Dpp, wingless (Wnt) and Hh molecules, resulting in the disruption of morphogen gradients (Belenkaya et al., 2004; Han et al., 2004; Kirkpatrick et al., 2004). In vertebrate development, the proteoglycan core-protein gene *glypican 3* (*Gpc3*) genetically interacts with *Bmp4* during limb development, and loss of Wnt signaling is also observed in mouse *Gpc3* mutants (Paine-Saunders et al., 2000; Song et al., 2005). By contrast, a mutation in the glycosaminoglycan biosynthetic gene *UDP-glucose dehydrogenase* (*Ugdh*) inhibited the signaling of FGF, but not of Nodal or Wnt3, in mesoderm- and endoderm-migration during gastrulation (Garcia-Garcia and Anderson, 2003). Another glycosaminoglycan biosynthetic gene, *Ext1*, is required for FGF8 signaling in CNS development, whereas a hypomorphic mutation in *Ext1* expanded the range of Indian hedgehog (Ihh) signaling during chondrocyte maturation (Inatani et al., 2003; Koziel et al., 2004). Interestingly, recent studies have shown that zebrafish *ext2* and *extl3* regulate Fgf10, but not Fgf4, signaling during limb development (Norton et al., 2005). These findings demonstrate the potential of HSPGs in regulating specific signaling pathways in a context-dependent manner.

The enzyme *N*-acetylglucosamine *N*-deacetylase-*N*-sulfotransferase (Ndst) catalyzes the first sulfation step during the synthesis of heparan sulfate. Consistent with its crucial role in HSPG modification, a *Drosophila Ndst* mutant, *sulfateless*, exhibited a segment-polarity phenotype as a result of impaired Wnt signaling (Lin and Perrimon, 1999). Furthermore, FGFR-dependent MAPK activity was also reduced in the *sulfateless* mutants during mesoderm and trachea development, and genetic interactions were demonstrated between *sulfateless* and the FGF-receptor gene (Lin et al., 1999). Finally, mosaic analysis showed that the loss of

[1]Department of Medical and Molecular Genetics, Indiana University of Medicine, Indianapolis, IN 46202, USA. [2]Department of Cellular and Molecular Medicine, Glycobiology Research and Training Center, University of California, San Diego, 9500 Gilman Drive, La Jolla, CA 92093, USA. [3]Department of General Zoology and Genetics, Westfälische Wilhelms-Universität Münster, Schlossplatz 5, 48149 Münster, Germany.

*Author for correspondence (e-mail: xz4@iupui.edu)

Accepted 4 October 2006

sulfateless prevented the diffusion of Dpp- and Hh-molecules in wing imaginal discs (Belenkaya et al., 2004; Han et al., 2004). These results established that Ndst genes are essential for the transport of morphogenic molecules and for their subsequent signaling.

There are four known Ndst enzymes in mammals, and biochemical experiments suggest that they might have different substrate specificities (Aikawa et al., 2001). Targeted deletion of *Ndst1* in mice resulted in embryonic lethality as a result of lung defects, whereas brain and ocular defects had also been noted (Fan et al., 2000; Grobe et al., 2005; Grobe et al., 2002; Ringvall et al., 2000). *Ndst2* mutants had impaired mast-cell development (Forsberg et al., 1999; Humphries et al., 1999), whereas the *Ndst3* mutant did not exhibit an obvious phenotype (Grobe et al., 2002). Importantly, *Ndst1* and *Ndst2* double-homozygous mutants exhibited early embryonic lethality, similar to that observed in *Ext1*- and *Ext2*-null mutants (Forsberg et al., 1999; Grobe et al., 2002; Lin et al., 2000; Stickens et al., 2005). These results demonstrate both the functional specificity and redundancy among the Ndst-family enzymes.

We have previously characterized cranial facial-developmental defects in *Ndst1* mutants and showed that *Ndst1* genetically interacted with *Shh*. In addition, we found that fibroblast cells derived from *Ndst1*-mutant embryos failed to respond to FGF stimulation in vitro, suggesting a role of *Ndst1* in FGF signaling (Grobe et al., 2005). In this study, we further examined lens development in *Ndst1* mutants, and demonstrated that loss of *Ndst1* function disrupted lens-vesicle invagination and lens cell differentiation. Importantly, we showed that BMP- and Wnt-signaling were not affected in *Ndst1*-mutant lenses. Instead, *Ndst1* loss of function led to a reduced binding of FGF ligand or FGF-FGFR complex on the cell surface. Consistent with this, MAPK signaling was downregulated during lens development. Therefore, *Ndst1* was important for lens-specific FGF signaling during development.

MATERIALS AND METHODS

Mice

Ndst1 mice were maintained in a C57BL/6 background (Grobe et al., 2005). *Bmp4* mice were kindly provided by Simon Conway (Indiana University School of Medicine, Indianapolis, IN, USA) and Bridget Hogan (Lawson et al., 1999). TOPGAL mice are obtained from Jackson Laboratory (DasGupta and Fuchs, 1999).

RT-PCR

Lens tissue was dissected in ice-cold PBS and immediately placed in liquid nitrogen. RNA was isolated from tissue extracts using a RNA-isolation kit (Qiagen, Valencia, CA), and reverse transcription was carried out according to the manufacturer's instructions (Invitrogen, Carlsbad, CA). The primers used for PCR were: *Ndst1* (forward: 5′-ACCACAGCC-AGCCAGAACGCTTGTG-3′; reverse: 5′-AGCTGCGCTCTTCCCCTT-TACTGTC-3′), *Ndst2* (forward: 5′-CCTTGCAGAACCGTTGTC-3′; reverse: 5′-CAGCCATTCCAATCCTG-3′), *Ndst3* (forward: 5′-TGT-GTTTCCTGTGAGTCCAGATGTGTG-3′; reverse: 5′-ATTGTCCTCCT-CACTTCCATCAGCCTG-3′) and *Ndst4* (forward: 5′-AACAGGAAAT-GACACTTATTGAAACG-3′; reverse: 5′-ACTTTGGGGCCTTTGGTA-ATATG-3′).

BrdU and TUNEL analysis

Pregnant mice were injected 2 hours prior to dissection with BrdU dissolved in PBS at 0.1 mg BrdU per 1 g body weight. The embryos were fixed in 4% PFA at 4°C overnight, incubated in 30% sucrose/PBS at 4°C overnight and embedded in OCT compound. Antigen retrieval was performed on 10 μm cryosections by microwave heating for 10 minutes at sub-boiling condition in citrate buffer at pH 6.0, and treated with 1 N HCl for 90 minutes at room temperature. Next, the sections were blocked with 10% normal goat serum in PBS at room temperature for 2 hours prior to the addition of an anti-BrdU antibody (Developmental Studies Hybridoma Bank, University of Iowa, Iowa City, IA, USA). After overnight incubation at 4°C, the sections were treated with secondary antibody and with the nuclear stain Hoechst for 2 hours at room temperature, and then examined under a Leica DM500 fluorescent microscope. The cell-proliferation rate was calculated as the ratio of BrdU-positive cells versus Hoechst-positives cells, and analyzed by the Student's *t*-test.

TUNEL staining was performed with an in situ cell-death detection kit (Roche, Indianapolis, IN, USA). Briefly, cryosections were processed for antigen retrieval as described above, incubated with blocking buffer (0.1 M Tris-HCl, pH 7.5, 3% BSA, 20% serum) for 30 minutes at room temperature and then with TUNEL reaction mixture for 2 hours at 37°C. After rinsing with PBS, the sections were blocked again with 0.05% blocking reagent (supplied in the TSA Indirect Tyramide Signal Amplification Kit, Perkin Elmer Life Science, Boston, MA, USA) for 30 minutes and then incubated with TUNEL-POD for 30 minutes at 37°C. Finally, the signal was developed with DAB substrate and detected under a Leica DM500 microscope.

RNA in situ hybridization

RNA whole-mount in situ hybridization was performed as previously described (Zhang et al., 2002). RNA in situ hybridization on sections was carried out according to a standard protocol (Dakubo et al., 2003). The following probes were used: *BF2*, *ERM* (from Bridget Hogan, Duke University Medical Center, Durham, NC, USA), *Hes1* (from Naoki Takahashi, Nara Institute of Science and Technology, Nara, Japan), *Math5* (also known as Atoh7 – Mouse Genome Informatics; from Tom Glaser, University of Michigan, Ann Arbor, MI, USA), *Ndst1*, *Pax6*, *Six3* (from Guillermo Oliver, St Jude Children's Research Hospital, Memphis, TN, USA) and *Sox2*. At least three embryos of each genotype were analyzed for each probe.

Erk-*P* and Smad1-*P* immunohistochemistry

X-gal staining, in situ hybridization and regular immunohistochemistry were performed as previously described (Zhang et al., 2003). Immunohistochemistry of phospho-Smad (Smad-*P*) and phospho-Erk (Erk-*P*) was carried out according to published procedures (Ahn et al., 2001). Briefly, mutant and control embryos were matched by somite numbers, and processed for coronal section on a Leica cryostat. For antigen retrieval, the sample slides were incubated in citrate buffer (10 mM sodium citrate, pH 9.0) at 80°C for 30 minutes, followed by treatment with 2% H_2O_2 to quench the endogenous peroxidase activity. After 1 hour of blocking at room temperature with 5% goat serum in PBS, the slides were incubated with primary antibody diluted in the blocking solution overnight at 4°C. Next, the slides were blocked for 30 minutes with 0.05% blocking reagent (TSA Indirect Tyramide Signal Amplification Kit, Perkin Elmer Life Science, Boston, MA, USA) and sequentially incubated with a biotin conjugated anti-rabbit antibody and ABC reagent (Vectastain ABC Kit, Vector Labs, Burlingame, CA, USA). To amplify the immunoperoxidase signal, the specimens were incubated with biotinyl tyramide diluted 1:50 in tyramide diluent for 10 minutes and then in 1:250 streptavidin-HRP for 30 minutes. Finally, the sections were incubated with DAB solution for color reaction.

As a control, we also performed phospho-Erk1/2 immunostaining on embryos treated with the FGFR1 inhibitor PD-173074 (a gift from Pfizer, New Jersey, NJ, USA) or the MAPK kinase inhibitor U0126 (Cell Signaling Technology, Beverly, MA). Prior to immunohistochemistry, the control embryos were incubated in RPMI containing 1% BSA; 50 μM U0126 or 40 μM PD-173074 at 37°C; and 5% CO_2 for 30 minutes. This effectively abolished the phospho-Erk1/2 expression in the embryos, thus validating the specificity of the phospho-Erk1/2 staining in our experiment (Corson et al., 2003).

The antibodies we used were: anti-phospho-Erk1/2, anti-phospho-Smad1/5/8, anti-phospho-Smad2 (all from Cell Signaling Technology, Beverly, MA, USA), anti-phospho-Smad1 (PS1) antibody [kindly provided by Peter ten Dijke (Leiden University Medical Center, Leiden, The Netherlands) and Carl-Henrik Heldin (Ludwig Institute for Cancer Research, Uppsala, Sweden)], anti-Pax6 (the Developmental Studies Hybridoma Bank, University of Iowa, Iowa City, IA, USA), anti-AP2α (Santa Cruz biotechnology, Santa Cruz, CA, USA), anti-Pax2, anti-Prox1 (both from Covance, Berkeley, CA, USA), anti-αA crystallin (kindly

provided by Samuel Zigler, National Institute of Health, Bethesda, Maryland, USA), anti-Six3 (kindly provided by Guillermo Oliver, St Jude Children's Research Hospital), and 10E4, HepSS-1 and 3G10 (all from Seikagaku, Tokyo, Japan).

FGF-ligand- and FGF-receptor-binding assay

Mutant embryos and their matched littermates were harvested and sectioned as above. Prior to the assay, the frozen sections were incubated in 0.5 mg/ml $NaBH_4$ for 10 minutes and then in 0.1 M glycine for 30 minutes. For analysis of FGF2 binding to heparan sulfate, the embryo sections were next quenched with 2% H_2O_2 and blocked with 0.05% TSA blocking reagent. Biotinylated FGF2 was produced as previously described (Bai et al., 1999) and incubated with the sections at 4°C overnight. The bound FGF2 was detected using a Vectastain ABC kit (Vector Labs, Burlingame, CA, USA) and stained in DAB solution (Sigma, St Louis, MO, USA). As a negative control, heparan sulfate on sections was degraded with 10 units of heparitinase I (Seikagaku, Tokyo, Japan) in 50 mM Tris-HCl pH 7.4, 50 mM sodium acetate, 1 mM calcium chloride and 1 mg/ml BSA at 37°C for 2 hours prior to the assay.

For in situ binding of the FGF-FGFR complex with heparan sulfate, we carried out the ligand and carbohydrate engagement (LACE) assay, as described (Allen and Rapraeger, 2003). Briefly, the frozen sections were incubated in 0.5 mg/ml $NaBH_4$ for 10 minutes, in 0.1 M glycine for 30 minutes and then blocked with 2% BSA. Next, the slides were incubated with 20 μM FGF, 20 μM human FGFR-Fc chimera (both from R&D Systems, Minneapolis, MN) and 10% fetal-calf serum in RPMI-1640 at 4°C overnight. After washing in PBS, the bound FGFR-Fc was detected using a cy3-labeled anti-human Fc IgG secondary antibody, and the fluorescence signal was examined using a Leica DM500 fluorescent microscope.

RESULTS

Ndst1 gene is expressed during lens development

To study the role of the *Ndst1* gene in eye development, we first examined its expression pattern by RNA in situ hybridization. Strong expression was detected in both the lens placode and in the optic vesicle in E9.5 mouse embryos (Fig. 1A). As a control, we also detected *Pax6* expression in the eye primordium, whereas no signal was observed with the *Ndst1* sense probe. This ubiquitous expression of *Ndst1* was also found in the later stages of eye development. At E12.5, *Ndst1* expression was present in the lens epithelia and in the retina. The specificity of RNA in situ hybridization was again demonstrated by the lack of signal using the *Ndst1* sense probe and the restricted staining pattern observed with the *Pax6* probe.

Next, we sought to confirm the in situ hybridization results by RT-PCR analysis. Total RNA was isolated from the lens and retina of E12.5 mice, and subjected to RT-PCR with specific primers for *Ndst1-4* and for the mitochondria ribosomal subunit *L19* (Fig. 1B). In the lenses, we detected the expression of *Ndst1* and, to a lesser extent, *Ndst2* only. By contrast, transcripts of all four Ndst genes were present in the retinae. As a control, similar levels of ribosomal subunit *L19* signals were observed in the retina and in the lens. Furthermore, no signal was detected in a RT-PCR reaction without reverse transcriptase. Previous studies have shown that *Ndst2*-null mice are normal, with the exception of defects in connective-tissue-type mast cells (Forsberg et al., 1999; Humphries et al., 1999). Together, these results suggest that, of the Ndst genes, *Ndst1* most probably plays the dominant role during lens development.

Inactivation of *Ndst1* disrupts eye development

We next examined homozygous *Ndst1*-null mice from E12.5 to E17.5 and observed ocular phenotypes in all embryos collected (n=18, Fig. 2A). Among them, four out of 18 embryos (22%) exhibited microphthalmia with reduced retinae and lenses, eight out of 18 embryos (44%) retained the retina but lacked lens, and the remaining six out of 18 embryos (34%) had no retina or lens. The size of embryos without lenses was indistinguishable from that of wild-type litter mates, whereas the embryos without eye structures were sometimes smaller and showed additional brain defects.

To investigate the origin of the ocular defects, we next analyzed homozygous *Ndst1* mutants at E13.5. The range of lens phenotypes was apparent in the *Ndst1*-mutant embryos and, even in the least-

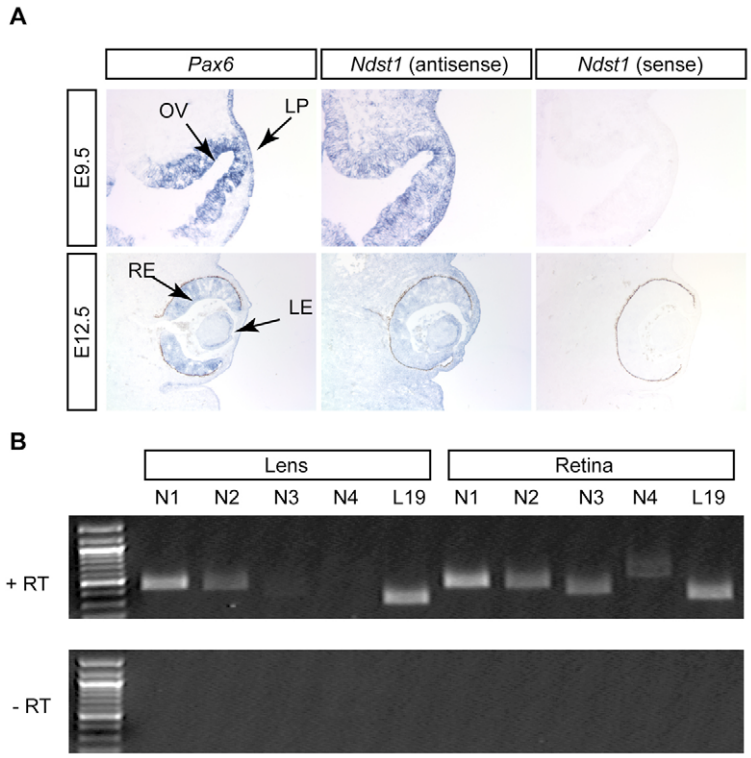

Fig. 1. *Ndst1* expression during lens development. (**A**) *Ndst1* is expressed in the developing eye. RNA in situ hybridization was performed on mouse embryonic sections. Lens placodes at E9.5 and lenses at E12.5 were both stained with a *Ndst1* antisense probe. As a control, samples were incubated with a *Ndst1* sense probe. The *Pax6* antisense probe specifically stained the developing lens placode (LP) and optic vesicle (OV) at E9.5, and lens epithelium (LE) and retina (RE) at E12.5. (**B**) RT-PCR analysis of Ndst gene expression in the lens and retina at E12.5. At this stage, only *Ndst1* (N1), *Ndst2* (N2) and mitochondria ribosomal subunit *L19* were detected in lens mRNA by RT-PCR, whereas all four Ndst genes were expressed in the retina. No signal was detected in the absence of reverse transcriptase (– RT). N3, *Ndst3*; N4, *Ndst4*.

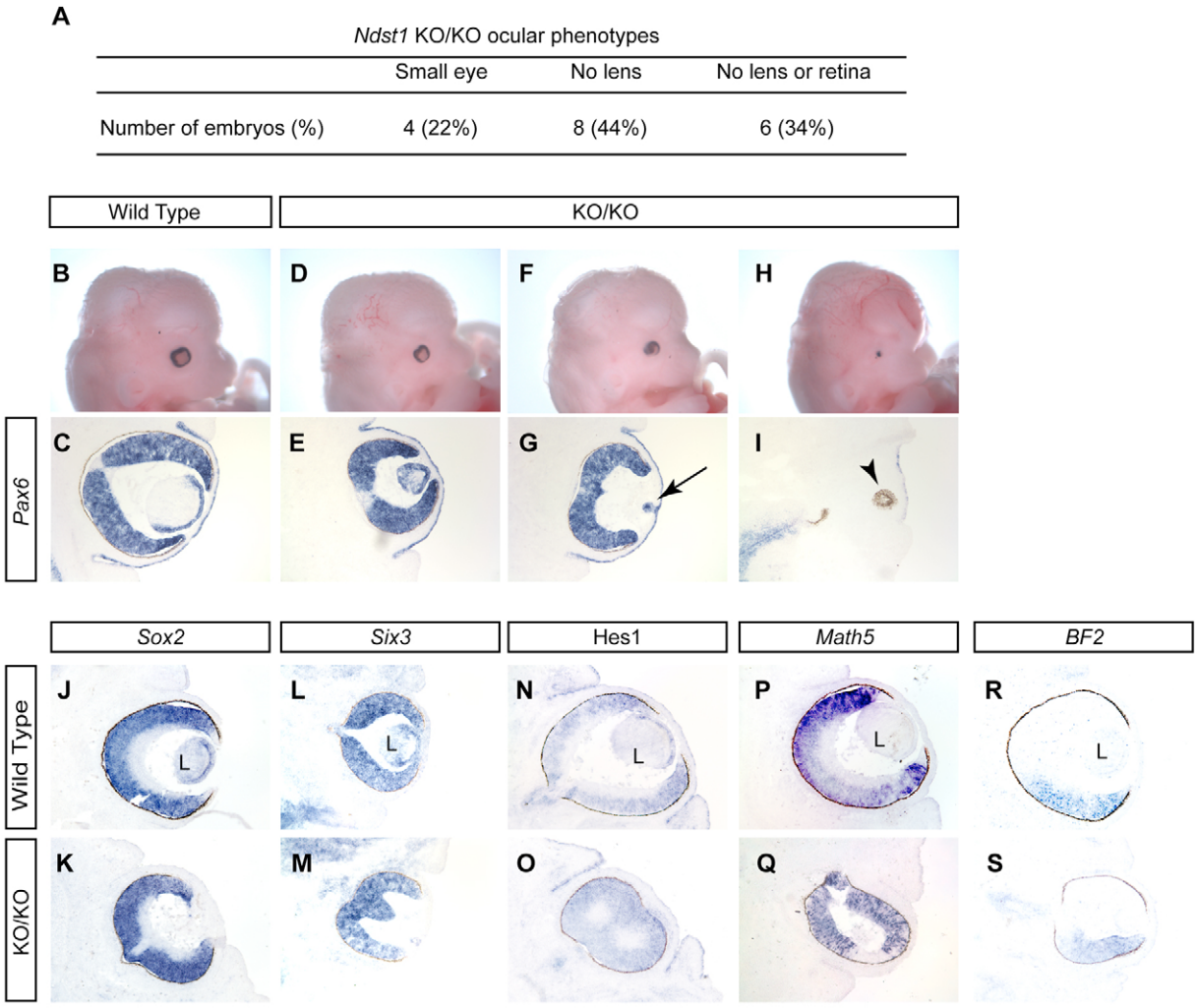

Fig. 2. *Ndst1*-mutant ocular phenotypes. (**A**) The range of ocular phenotypes observed in E12.5 to E17.5 *Ndst1*$^{KO/KO}$ embryos. (**B-I**) E13.5 *Ndst1* embryos and eye sections showing *Pax6* RNA in situ staining. Severe lens-developmental defects were observed in E13.5 *Ndst1*-mutant embryos (D-I), ranging from small or absent lenses to a complete lack of eyes. (**J-S**) Retinal patterning in the *Ndst1* mutant. RNA in situ hybridization was performed on E14.5 embryos. *Sox2*, *Six3*, *Hes1*, *Math5* and *BF2* were expressed in both wild-type and *Ndst1*$^{KO/KO}$ retinae. Notice the lack of lenses in *Ndst1*$^{KO/KO}$ eyes. KO/KO, homozygous *Ndst1*-knockout embryos; L, lens.

affected embryos, lenses were smaller and pinched at the anterior region (Fig. 2D,E). Unlike the wild-type littermates, the lens lumen of which was mostly filled with lens fibers, much of the anterior-lens vesicle was still empty in mutant lenses. To uncover the molecular changes in *Ndst1* mutants, we also performed RNA in situ hybridization on frozen sections to stain for *Pax6* gene expression (Fig. 2B-I). *Pax6* expression should be restricted to the epithelial cells of the lens at this stage; however, in mutants, *Pax6* transcripts were detected throughout the lens (Fig. 2E). In more-severely affected mutants, the entire lens was reduced to a small cluster of cells connected to the surface ectoderm with a residual lens stalk (Fig. 2G, arrow) and the retinae were mis-shaped. Finally, some *Ndst1* mutants lacked any apparent retina or lens structure (Fig. 2H). There were sometimes pigmented cells left at the presumptive eye region (Fig. 2I, arrowhead). Interestingly, *Pax6* expression could still be detected in the surface ectoderm (Fig. 2I). The severity of the lens defects observed in these E13.5 *Ndst1* embryos suggested that failure of lens development probably originated even earlier during development.

We next asked whether the *Ndst1*-mutant eye phenotype was restricted to the lens (Fig. 2J-S). *Sox2* is a major early neural marker during development; *Six3*, *Hes1* and *Math5* are transcription factors that define retinal progenitor cells; and, finally, *BF2* marks the posterior region of the retina in topographic axon mapping (Brown et al., 2001; Darnell et al., 1999; Furukawa et al., 2000; Wang et al., 2001; Yuasa et al., 1996; Zhu et al., 2002). RNA in situ hybridization showed that transcripts of these genes were present in both wild-type and *Ndst1*-mutant retinae. Therefore, retinal patterning and differentiation appeared to have at least been initiated in the absence of the lens in *Ndst1* mutants.

Early lens defects in *Ndst1*-knockout embryos

In search of the mechanism for lens defects, we next studied lens induction in *Ndst1* mutants. At the 24-somite stage, the mutant lens placode was morphologically indistinguishable from wild-type controls (Fig. 3A). However, at the 30-somite stage, wild-type embryos had formed the lens pit, whereas *Ndst1*-mutant embryos exhibited less-advanced indentation in the lens placode

(Fig. 3A). At the 35-somite stage (E11.0), lens vesicles were either entirely absent (data not shown) or reduced in size in *Ndst1* mutants (Fig. 3A). Throughout lens-vesicle development, the rates of BrdU incorporation in mutant embryos were consistently reduced in comparison to wild-type controls (Fig. 3B). By contrast, few apoptotic cells were observed in either wild-type or *Ndst1*-mutant lens vesicles (Fig. 3C, arrow), even though there was a significant increase in TUNEL staining in periocular mesenchyme in *Ndst1*-mutants (Fig. 3C, arrowhead). These results suggest that *Ndst1* mutants were defective in lens cell proliferation.

We next studied the molecular defects underlying lens induction in *Ndst1* mutants. *Pax6* and *Six3* are crucial transcription factors for lens induction and morphogenesis that are expressed at increasing levels as the lens placode invaginates to form the lens vesicle. At the 26- and 28-somite stages (E10.5), mildly affected *Ndst1*-mutant embryos also expressed the Pax6 and Six3 proteins at high levels (Fig. 4B,E, arrows); however, the expressions of these proteins were less elevated in severely affected mutants (Fig. 4C,F, arrowheads). Of note, we did not observe a reduction in *Pax6* expression after lens-placode invagination, suggesting that *Ndst1* is specifically required for *Pax6* expression during lens induction (Fig. 4G-O). Although the disruption of Pax6 and Six3 expressions could be secondary to lens-development failure, it may also directly contributes to lens-induction defects in *Ndst1* mutants.

AP2α, a transcription factor required for lens development, was found to be expressed in both wild-type and *Ndst1*-mutant lens primordia at the 32-somite stage (data not shown). In 35-somite embryos, however, some of the *Ndst1* mutants expressed AP2α in overlying head ectoderm only, and not in lens vesicles (Fig. 4I, five out of eight embryos). Therefore, AP2α expression was specifically lost between the 32- and 35-somite stages. Normally, αA crystallin is expressed in the lens pit at E10.5 and *Prox1* expression initiates in the lens placode at E9.5 (Robinson and Overbeek, 1996; Wigle et al., 1999). None of these molecules were observed in the more severely affected homozygous *Ndst1*-null mutants (Fig. 4L, four out of six mutants for Prox1; Fig. 4O, two out of three mutants for αA crystallin). Notice that some *Ndst1* mutants exhibited relatively mild lens-vesicle defects and that these embryos also preserved Pax6, AP2α, Prox1 and αA crystallin expressions. This is consistent with the observation that *Ndst1* mutants displayed a range of phenotypes, including some that developed both lens and retina. Taken together, these molecular defects show that *Ndst1* inactivation results in a delay or even failure of lens-vesicle development.

Ndst1 knockout did not affect canonical BMP and Wnt signaling in the lens

BMP/TGFβ signaling are known to play important roles in lens development. We thus examined the intracellular mediators of BMP/TGFβ signaling – the phospho-Smad1 (Smad1-*P*) and phospho-Smad2 (Smad2-*P*) proteins – in *Ndst1*-mutant lenses. To validate the Smad1-*P* antibody, we first compared its staining pattern in wild-type and *Bmp4*-mutant embryos. Consistent with previous reports, we observed specific Smad1-*P* expression in the first branchial arch (Fig. 5A, arrowhead) and olfactory placode (Fig. 5A, arrow) at E9.5 (Ahn et al., 2001; Faber et al., 2002). Not surprisingly, this coincides with strong *Bmp4* expression in these locations (Dudley and Robertson, 1997). In *Bmp4*-knockout embryos, however, this Smad1-*P* staining pattern was abolished. Therefore, Smad1-*P* immunohistochemistry reliably detected active Bmp4 signaling during embryonic development.

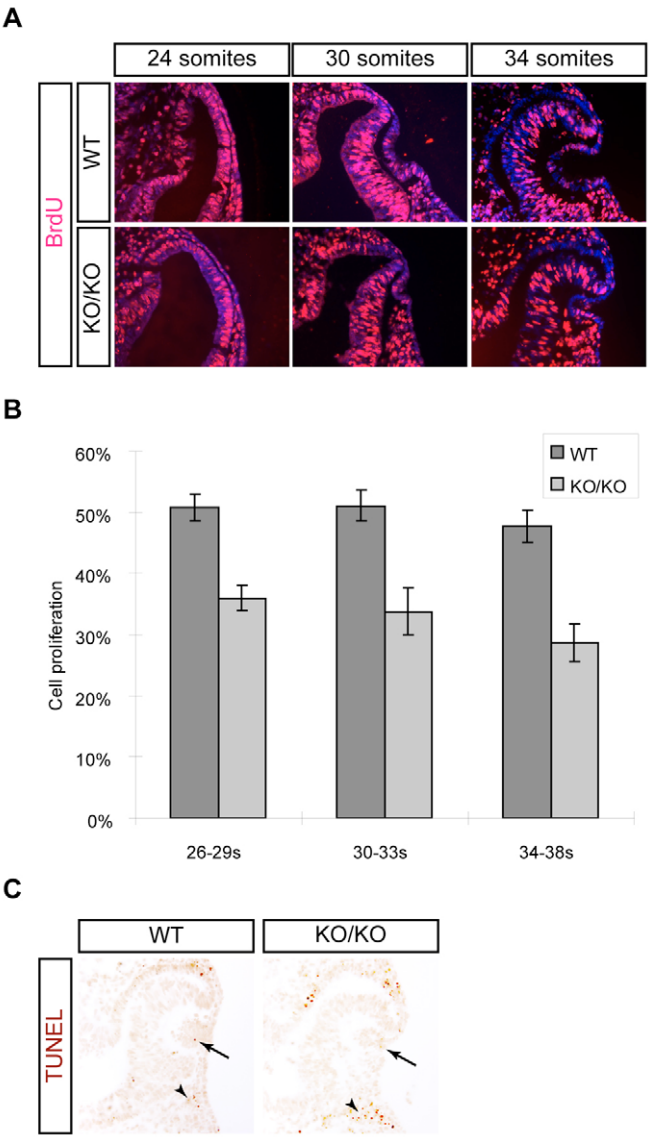

Fig. 3. Lens cell proliferation defects in *Ndst1* mutants. (**A**) Homozygous *Ndst1*-knockout embryos and wild-type controls were stained for BrdU (red), and the nuclei were counterstained with Hoechst at the 24-, 30- and 34-somite stages. (**B**) Cell proliferation was quantitated as the ratio of BrdU-positive cells versus Hoechst-positives cells at different stages of development [26- to 29-somite (s) stages; 30- to 33-s stages; and 34- to 38-s stages]. There was a consistent reduction of cell proliferation in *Ndst1*-mutant lenses compared with wild type (Student's *t*-test: 26- to 30-somite stages, $P<0.001$; 30- to 34-somite stages, $P<0.01$; 34- to 38-somite stages, $P<0.001$. At least four embryos were analyzed for each genotype at each stage). (**C**) Lack of apoptosis defects in *Ndst1*-mutant lens vesicles. TUNEL staining in *Ndst1* mutants was normal in the lens vesicle (arrows), but increased in periocular mesenchyme (arrowheads). KO/KO, homozygous *Ndst1*-knockout embryos; WT, wild type.

In wild-type embryos, Smad1-*P* was present in the presumptive lens ectoderm and optic vesicle as early as the 20-somite stage (E9.5), forming an anterior-posterior gradient (Fig. 5B). This expression pattern persisted in 30 somite-stage embryos (E10.5) as lens placodes invaginated. In homozygous *Ndst1*-knockout embryos (KO/KO), similar Smad1-*P* staining was detected, even as the lens-

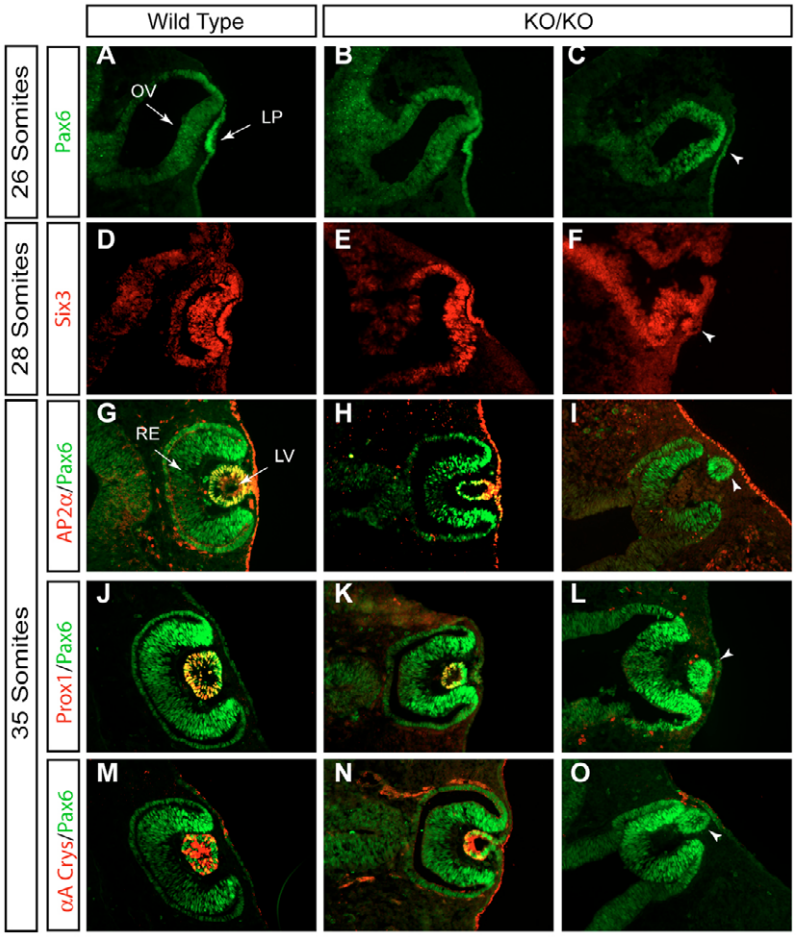

Fig. 4. Expression of lens-specific genes in *Ndst1* mutants. (**A-F**) At the 26- to 28-somite stage, Pax6 and Six3 were detected in the lens placode (LP), but the level of their expression was reduced in severely affected *Ndst1* mutants (arrowhead). (**G-O**) Molecular defects in *Ndst1*-mutant lens vesicles at the 35-somite stage. As the lens vesicles invaginated, expression of AP2, Prox1 and αA crystallin was downregulated in severely affected mutant lens vesicles (arrowheads in I,L,O). Notice that AP2α expression was still detectable in the overlying ectoderm and Pax6 expression was not perturbed. OV, optic vesicle; LP, lens placode; LV, lens vesicle; RE, retina.

vesicle formation was disrupted (Fig. 5B, arrowhead). Furthermore, both wild-type and *Ndst1*-mutant lens vesicles strongly expressed the Smad2-*P* protein at E11.0 (Fig. 5B, arrow). Therefore, the BMP/TGFβ signaling mediated by phospho-Smad proteins was unaffected in *Ndst1* mutants. To further test the genetic interaction between *Ndst1* and *Bmp4*, we crossed *Ndst1* mice with a *Bmp4*-mutant strain carrying a *LacZ* knock-in allele ($Bmp4^{LacZ}$) (Lawson et al., 1999). As shown in Fig. 5C, the loss of one copy of the *Bmp4* gene did not enhance the lens phenotype in either heterozygous or homozygous *Ndst1*-mutant embryos (n=24 for $Ndst1^{KO/+}$ $Bmp4^{LacZ/+}$, n=10 for $Ndst1^{KO/KO}$ $Bmp4^{LacZ/+}$), and the *Bmp4* expression reported by the β-galatosidase activity was also unchanged in the *Ndst1*-mutant background. Taken together, these results suggest that BMP/TGFβ signaling was not affected by *Ndst1* inactivation in the lens.

Canonical Wnt signaling results in the inhibition of GSK-3β kinase and in the accumulation of β-catenin in the nucleus, which allows TCF-family transcription factors to activate downstream target genes. Using a transgenic mouse line carrying a *LacZ* reporter driven by multimerized TCF after activation by β-catenin (TOPGAL) (DasGupta and Fuchs, 1999), we also assayed the canonical Wnt signaling activity in *Ndst1*-mutant lenses (Fig. 5D). In both wild-type and *Ndst1*-mutant embryos, similar TOPGAL transgene expressions were observed in periocular tissue, whereas no β-galatosidase activity was detected in the lens. Therefore, the lens defects in *Ndst1* mutants are unlikely to be caused by abnormal canonical Wnt signaling.

Ndst1 mutants are defective in heparan sulfate synthesis and FGF-FGFR binding

We next analyzed the expression pattern of heparan sulfate during lens development. The monoclonal antibody 10E4 recognizes an epitope unique to heparan sulfate, whereas the HepSS-1 antibody binds to *N*-sulfated heparan sulfate domains (Leteux et al., 2001; van den Born et al., 2005). In wild-type embryos, both antibodies stained the basal membranes of the optic vesicle and the lens vesicle (Fig. 6). We further demonstrated that this staining pattern was specific to heparan sulfate because sections treated with heparitinase I completely lost the staining (Fig. 6). Heparitinase I digestion also generated a heparan sulfate 'stub' motif, which was the epitope of the 3G10 antibody (David et al., 1992). In heparitinase I-treated sections, we observed specific 3G10 staining in the developing eye (Fig. 6). Therefore, heparan sulfate was abundantly expressed during lens formation.

Ndst1 catalyzes the *N*-deacetylation and *N*-sulfation of heparan sulfate. Interestingly, we observed a complete loss of 10E4 and HepSS-1 staining in KO/KO embryos, but 3G10 staining after the Heparitinase I treatment remained intact (Fig. 6). Because the 3G10 antibody detects heparan sulfate stubs that remain after heparitinase digestion, these findings indicate that heparan sulfate chains were still being made in the *Ndst1*-mutant embryos, but that these were undersulfated.

The sulfation pattern of heparan sulfate is important for its interaction with FGF ligands and receptors. We thus performed LACE assays and asked whether *Ndst1* mutants defective in heparan

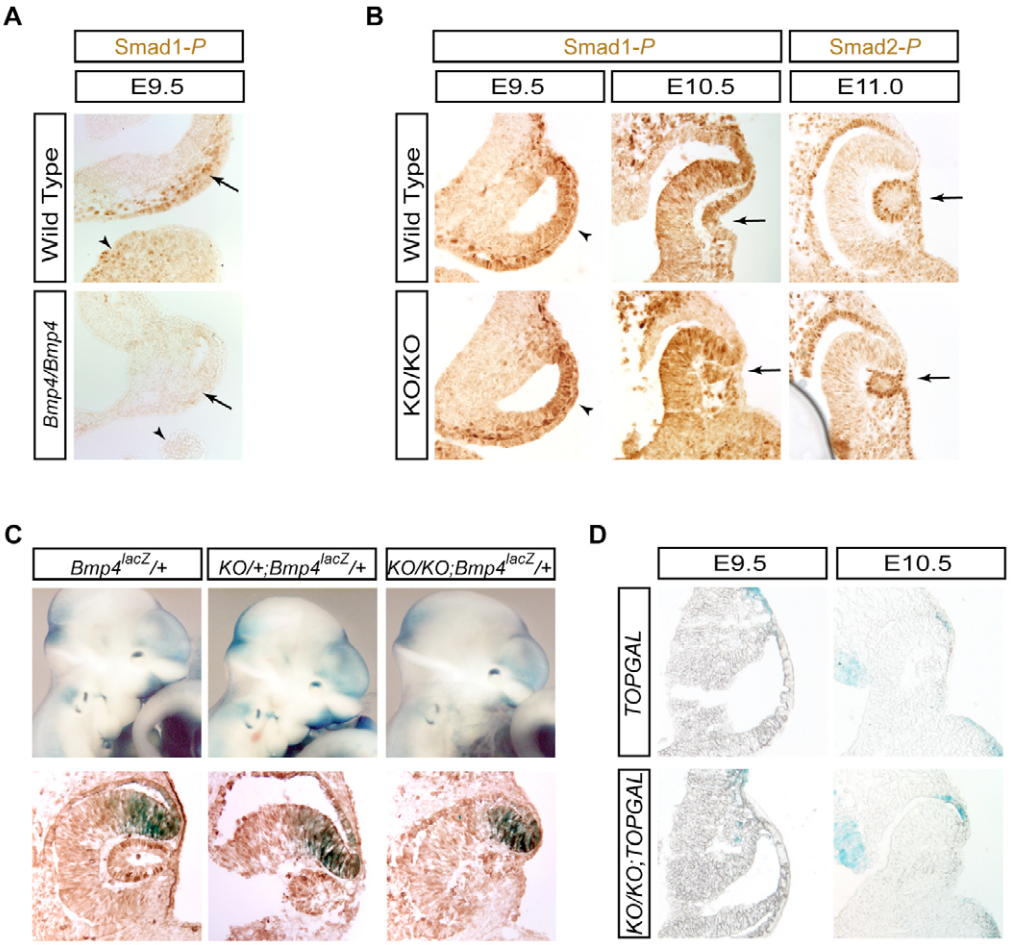

Fig. 5. BMP- and Wnt-signaling were unaffected by *Ndst1* inactivation. (**A**) Detection of BMP signaling by Smad1-*P* immunohistochemistry. Smad1-*P* was observed in E9.5 wild-type nasal mesenchyme (arrow) and branchial arches (arrowhead), but not in *Bmp4*-mutant embryos. (**B**) Smad1-*P* and Smad2-*P* expressions were not affected in *Ndst1*-mutant lenses. In both wild-type and mutant embryos, Smad1-*P* and Smad2-*P* was expressed at similar levels in the lens. The same section used for Smad1-*P* staining was also probed with Pax6 and Pax2 antibodies to visualize the lens vesicle. Arrows indicate lens placode; arrowheads indicate lens vesicle. (**C**) Lack of genetic interaction between *Bmp4* and *Ndst1*. Addition of the $Bmp4^{LacZ}$ allele did not affect the lens phenotype in *Ndst1*-mutant eyes (upper panels). Furthermore, *Bmp4* expression, as indicated by a knock-in *LacZ* reporter, was unchanged in the *Ndst1* mutant (lower panels). (**D**) Canonical Wnt signaling indicated by TOPGAL reporter activity was not perturbed by *Ndst1* inactivation during lens development. KO/KO, homozygous *Ndst1*-knockout embryos.

sulfate modification also exhibited reduced FGF binding (Allen and Rapraeger, 2003). Embryo sections were incubated with FGF2 tagged with biotin and the binding of FGF2 to eye tissue was detected by biotin histochemistry. In wild-type eyes, biotinylated FGF2 was specifically localized at the basal membrane of lens- and retinal-cells, and the FGF2-binding pattern closely resembled the distribution of endogenous heparan sulfate during eye development (Fig. 7A). As a control, no staining was observed in the absence of biotinylated FGF2 (data not shown). More importantly, prior treatment of embryo sections with heparitinase I completely abolished the staining (Fig. 7A). This demonstrates that the binding of biotinylated FGF2 on these tissue sections crucially depends on intact heparan sulfate. In *Ndst1*-mutant embryos, incubation with the same concentration of biotinylated FGF2 resulted in much-weaker staining as compared with the wild-type controls, and significant binding of FGF2 to lens cells was observed only after a 10-fold increase in FGF2-ligand concentration (Fig. 7A). Therefore, the *Ndst1* mutation resulted in a reduced affinity of FGF2 to the lens cell basement membrane.

We next tested whether the assembly of the FGF-FGFR complexes was also affected in *Ndst1* mutants. For this experiment, we assayed FGF8, which has been shown to be important for early eye development, and FGF19, the mouse homolog of which (FGF15) is strongly expressed in the optic vesicle (Lovicu and Overbeek, 1998; McWhirter et al., 1997; Vogel-Hopker et al., 2000). Eye sections from E10.5 embryos were incubated with purified FGF and with FGFR fused with the human IgG Fc domain (FGFR-Fc), and bound FGFR-Fc was probed with an anti-IgG antibody. In wild-type-embryo sections, we observed specific binding of FGFR2c and FGFR3c to lens- and retina-cells in the presence of FGF8b (Fig. 7B). As a control, no signal was detected without FGF8b or after the treatment of tissue sections with heparitinase I (data not shown). This demonstrated that the observed FGFR binding in situ was mediated by FGF and cell-surface heparan sulfate. In E10.5 *Ndst1*-mutant sections, binding of FGFR3c-FGF8b was reduced throughout the eye region (Fig. 7B). In comparison, FGFR2c-FGF8b binding was weaker in the retina (Fig. 7B, arrow) and became almost undetectable in the

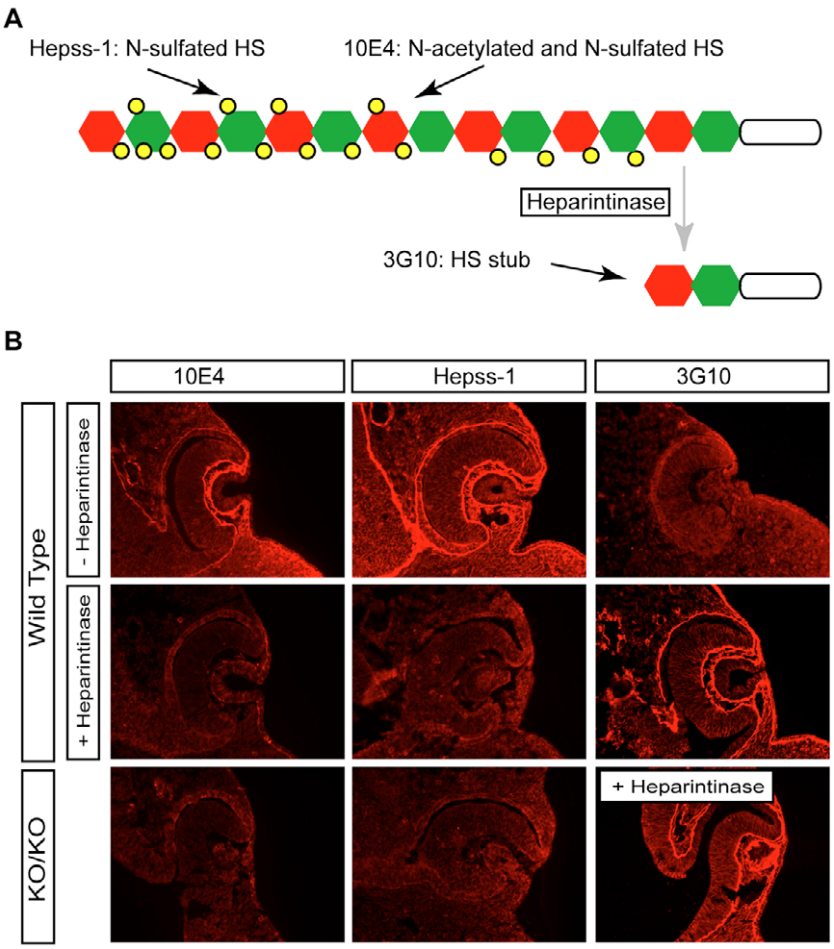

Fig. 6. Disruption of heparan sulfate synthesis in *Ndst1* mutants. (**A**) Specificities of Hepss-1, 10E4 and 3G10 heparan sulfate antibodies. (**B**) Loss of sulfation of heparin sulfate in KO/KO embryos. Hepss-1 and 10E4 antibodies were specific for heparan sulfate. Their staining in the developing lens was lost both in heparitinase I-treated (+ Heparitinase) wild-type embryos and in *Ndst1* mutants. By contrast, staining by 3G10 antibody detected the heparan sulfate stub region after heparitinase I cleavage. Staining was observed in both wild-type and mutant embryos. KO/KO, homozygous *Ndst1*-knockout embryos.

Ndst1-mutant lens (Fig. 7B, arrowhead). The more-pronounced loss of FGFR2c-FGF8b binding to the lens was especially interesting considering the significant lens phenotype in *Ndst1* mutants. Finally, FGFR4-FGF19 exhibited weak but unchanged binding to both wild-type and *Ndst1*-mutant eyes, suggesting that *Ndst1* inactivation disrupted the assembly of some, but not all, FGF-FGFR pairs in the eye tissues.

Based on previous reports of FGF expression patterns, we extended our analysis to FGF1, 2, 3, 5, 8, 9 and 15 to assay their pair-wise interactions with FGFR1b, 1c, 2b, 2c, 3b, 3c and 4 (Chow and Lang, 2001; de Iongh and McAvoy, 1993; Kitaoka et al., 1994; Lovicu and Overbeek, 1998; Martinez-Morales et al., 2005; McWhirter et al., 1997; Nguyen and Arnheiter, 2000; Vogel-Hopker et al., 2000; Zhao et al., 2001). This includes all the FGF and FGFR variants known to be present during early eye development. It also represents all six subfamilies of FGFs, except the FGF11-14 subfamily, which does not interact with FGF receptors. In wild-type embryos, the binding of each FGF-FGFR pair largely confirmed previous results obtained in cell culture or in biochemical studies (Fig. 7C). In *Ndst1* mutants, however, FGF-FGFR interactions were altered. Except for FGF19, the interaction of each FGF with at least one FGFR variant was disrupted by *Ndst1* deletion. Different FGF-FGFR pairs were affected differentially by *Ndst1* inactivation, and each pair exhibited distinct binding activities in different tissues (Fig. 7C and data not shown). Overall, 18 FGF-FGFR pairs required Ndst1 function in the lens, suggesting that Ndst1-modified heparan sulfate potentially regulates a large number of FGF-FGFR interactions during lens development.

FGF-signaling targets were downregulated in *Ndst1* mutants

The significant loss of in situ FGF-FGFR binding to *Ndst1*-mutant tissue raised the possibility that FGF signaling was compromised during eye development. To test this idea, we first examined the expression of the phospho-Erk1/2 (Erk-*P*) proteins – the downstream effectors of the FGF-MAPK pathway. Using a phospho-specific antibody against Erk1/2, we detected Erk-*P* expression in the developing optic cup and lens vesicle in E10.5 embryos (Fig. 8A). The specificity of the immunohistochemistry assay was demonstrated in embryos cultured in the presence of the MEK inhibitor U0126, which acts upstream of Erk1/2 (Favata et al., 1998). After treatment, Erk-*P* expression was completely lost throughout the embryos, including the eye tissues (Fig. 8A). Furthermore, we cultured wild-type embryos with PD173074, a potent FGFR inhibitor (Skaper et al., 2000). This treatment also abolished Erk-*P* staining in the developing optic cup and lens vesicle (Fig. 8A). Together, these results confirm previous reports that Erk-*P* expression directly correlates with FGFR-MAPK signaling activity during eye development (Corson et al., 2003; Govindarajan and Overbeek, 2001; Lovicu and McAvoy, 2001).

In wild-type embryos, strong Erk-*P* immunostaining was observed in lens placodes at the 27-somite stage, whereas little Erk phosphorylation was detected in the *Ndst1*-mutant lens ectoderm (Fig. 8B, arrowhead). Similarly, wild-type embryos exhibited strong Erk-*P* expression in the invaginating lens vesicle at the 30- and 32-somite stages. In mutant embryos, where lens development failed to progress beyond initial lens-placode invagination, the lens tissues

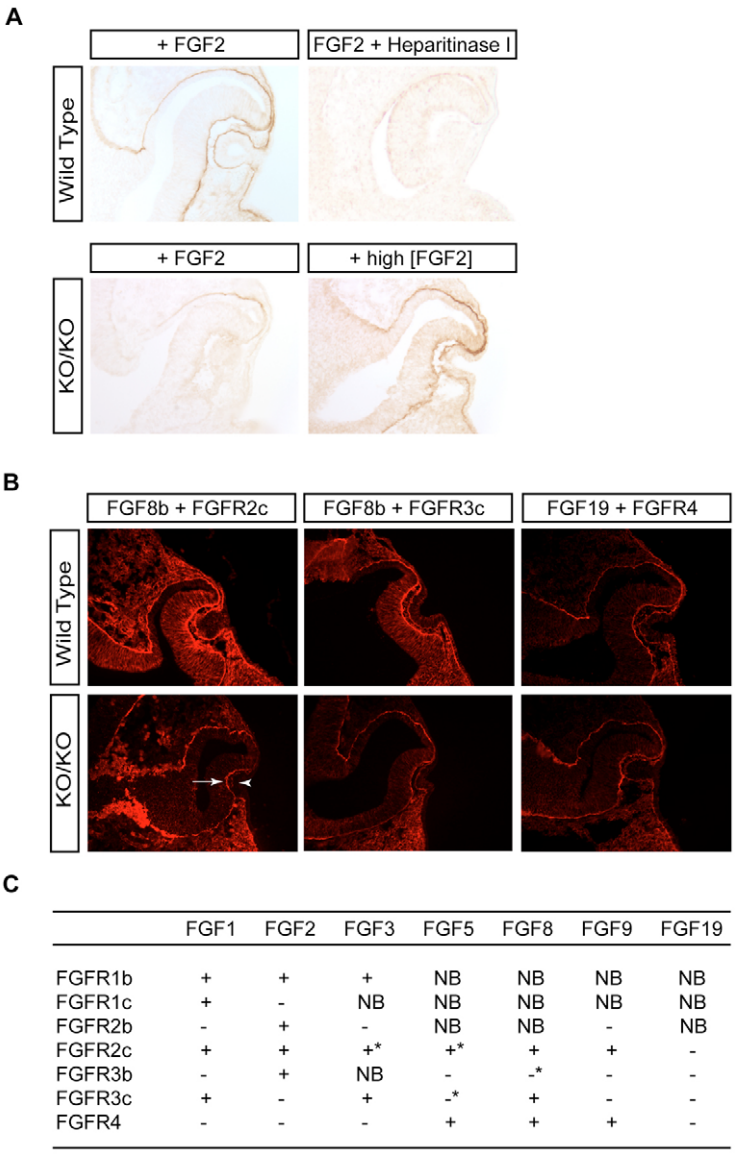

C

	FGF1	FGF2	FGF3	FGF5	FGF8	FGF9	FGF19
FGFR1b	+	+	+	NB	NB	NB	NB
FGFR1c	+	-	NB	NB	NB	NB	NB
FGFR2b	-	+	-	NB	NB	-	NB
FGFR2c	+	+	+*	+*	+	+	-
FGFR3b	-	+	NB	-	-*	-	-
FGFR3c	+	-	+	-*	+	-	-
FGFR4	-	-	-	+	+	+	-

Fig. 7. Reduction of FGF and FGFR binding to the *Ndst1* lens. (**A**) Reduced FGF2 binding to *Ndst1*-mutant embryos. Biotinylated FGF2 (1:10,000 dilution) was incubated with lens sections and assayed by immunohistochemistry in wild-type embryos. Significant FGF2 binding in the *Ndst1* mutant was observed only with high concentrations of FGF2 (1:1000 dilution). (**B**) Diminished FGF-FGFR binding on *Ndst1*-mutant lenses. *Ndst1*-mutant lenses exhibited reduced binding to FGF8b-FGFR2c and FGF8b-FGFR3c, whereas FGF19-FGFR4 remained the same for wild-type and mutant embryos. (Arrow indicates weaker staining in retina; arrowhead indicates strongly reduced staining in lens.) (**C**) Requirement of Ndst1 for multiple FGF-FGFR interactions. *Ndst1* mutation disrupts some of the FGF-FGFR interactions on the cell surfaces of the lens (+), but not others (–). *Weak binding. NB, no binding. KO/KO, homozygous *Ndst1*-knockout embryos.

expressed Pax6 but not the Erk-*P* proteins (Fig. 8B, arrow). Interestingly, strong expression of Erk-*P* remained in the mutant optic vesicle throughout development. These results show that the MAPK pathway was specifically disrupted in the *Ndst1*-mutant lens.

Downstream to FGF-MAPK signaling, ETS-domain transcription factors are both transcriptional effectors and direct targets of the pathway (Tsang and Dawid, 2004). In particular, previous experiments have demonstrated that the expression of the Pea3 (also known as Etv4 – Mouse Genome Informatics) group of ETS-domain transcription factors [ER81 (also known as Etv1 – Mouse Genome Informatics), ERM (also known as Etv5 – Mouse Genome Informatics) and Pea3] closely mimic FGF-signaling activities (Munchberg and Steinbeisser, 1999; Raible and Brand, 2001; Roehl and Nusslein-Volhard, 2001). Using RNA in situ hybridization, we observed expression of *ERM* in developing wild-type lens vesicles at E10.5. By contrast, *ERM* expression was significantly downregulated in *Ndst1*-mutant lenses. Consistent with lens-specific loss of Erk-*P*, the reduction of *ERM* was also confined to the developing lens, because midbrain- and branchial-arches still exhibited strong *ERM* expression. Together, these results show that FGF-MAPK signaling was disrupted in the *Ndst1*-mutant lens.

DISCUSSION

An interesting finding in this study was that *Ndst1* inactivation disrupted signaling of FGF, but not of BMP or Wnt, during lens development. This is surprising considering that the *Drosophila* Ndst gene *sulfateless* is essential for all three signaling pathways. It is possible that specific heparan sulfate modifications generated by Ndst1 are only required for FGF signaling, but not for BMP/Wnt signaling. However, another explanation may be that FGF signaling is more sensitive to defective heparan sulfate than the other two signaling pathways. In BMP/Dpp- and Wnt-signaling, heparan sulfate may be required primarily for morphogen movement in the developing field (Lin, 2004). Thus, in *Drosophila* tissue where *Dpp* is abundantly expressed, heparan sulfate mutation has no obvious effect on Dpp-controlled patterning (Haerry et al., 1997; Lin and Perrimon, 1999). By contrast, cell-surface heparan sulfate acts as a co-receptor for FGF signaling, forming a trimeric complex with FGF and the FGF receptor. Therefore, all mutant cells deficient for heparan sulfate fail to respond to FGF signaling. In vertebrate lens development, the lens vesicle develops from a single layer of placodal cells, which is directly exposed to strongly expressed inductive signals, such as BMP4, from the optic vesicle. It is therefore expected

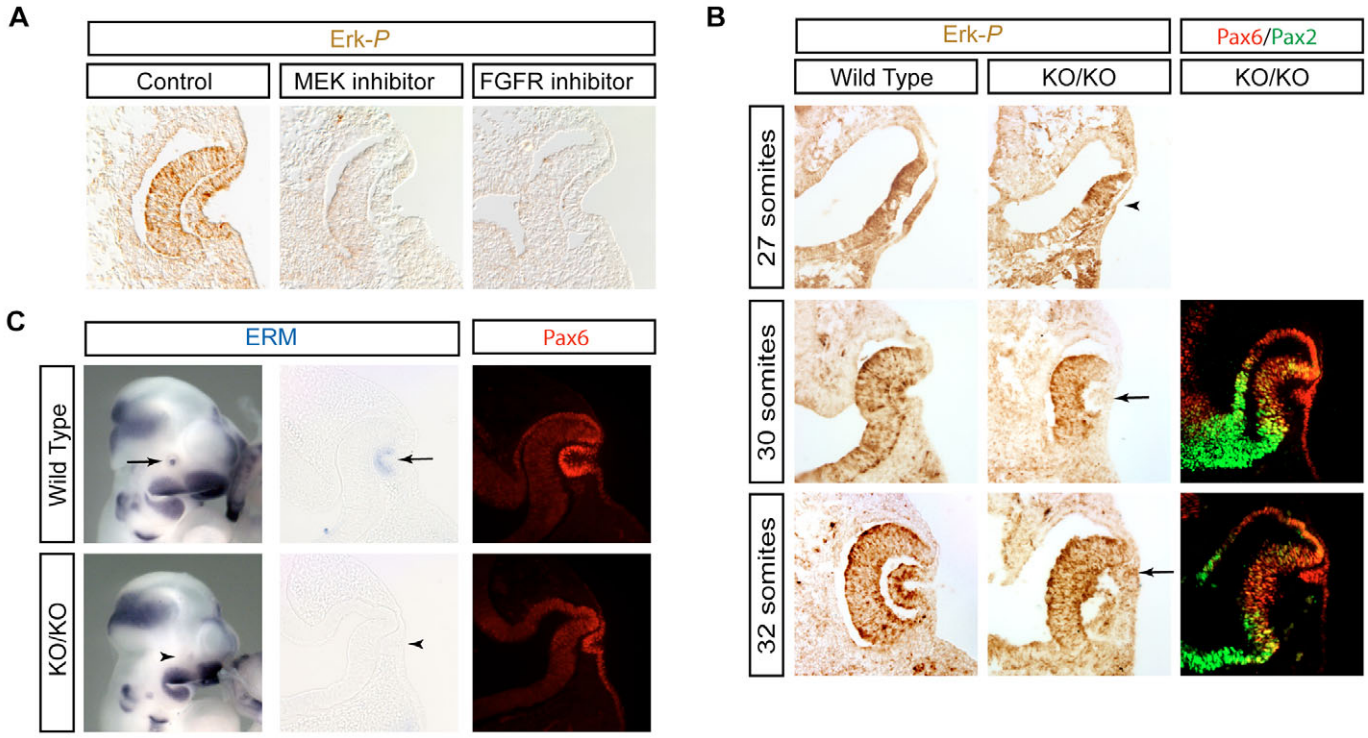

Fig. 8. Loss of FGF signaling in *Ndst1*-mutant lenses. (**A**) Specific Erk-*P* staining in the developing lens. Erk-*P* was detected in control lenses, but not in embryos treated with MEK- or FGFR-inhibitors. (**B**) Loss of Erk-*P* expression in *Ndst1*-mutant lenses. Erk-*P* immunostaining was decreased in the *Ndst1*-mutant lens placode (arrowhead) and lens vesicle (arrow), whereas Pax6 and Pax2 expressions were preserved. (**C**) The FGF-responsive transcription factor *ERM* was downregulated in the E10.5 *Ndst1* mutant. RNA in situ hybridization showed that *ERM* was expressed in wild-type, but not in *Ndst1*-mutant, lenses. The lens vesicle was identified by Pax6 staining the same section. KO/KO, homozygous *Ndst1*-knockout embryos.

that the *Ndst1*-mutant lens vesicle will maintain its BMP response. By contrast, heparan sulfate is required for FGF-signal binding on the cell surface, and *Ndst1* inactivation will thus abrogate the FGF-signaling activity during lens-vesicle development.

Ndst1 also exhibited remarkable specificity in regulating FGF-FGFR interactions. Previous studies have shown that *N*-sulfation of heparan sulfate is essential for its binding to FGF2 (Turnbull et al., 1992). Consistent with this model, we observed reduced FGF2 binding to lens cells in *Ndst1* mutants. In addition, *Ndst1* inactivation significantly reduced binding of lens cell heparan sulfate to FGF8b-FGFR2c and FGF8b-FGFR3c complexes. Surprisingly, the binding affinity of FGF19-FGFR4 to lens cell heparan sulfate remained unchanged in *Ndst1* mutants. This suggested that Ndst1-mediated structural remodeling of heparan sulfate was necessary to allow for the assembly of some, but not all, FGF-FGFR complexes on the cell surface. Such distinct requirement for heparan sulfate motifs in FGF signaling has also been observed in earlier studies (Ford-Perriss et al., 2002). In particular, a mutation in the *heparan sulfate 2-O-sulfotransferase* (*HS2ST*) gene was shown to disrupt binding of FGF8b-FGFR2c, but not FGF8b-FGFR3c, on E10.5 heart sections (Allen and Rapraeger, 2003). In zebrafish limb development, *ext2* and *extl3* mutants specifically affected FGF10, but not FGF4, signaling (Norton et al., 2005). Taken together, these results suggest that heparan sulfate-synthesizing enzymes can play an active role in regulating different FGF-signaling pathways.

In this study, we have systematically analyzed in situ FGF-FGFR binding on the cell surface of the lens. Our results are mostly consistent with mitogenesis studies performed in cell culture and with binding studies by surface plasmon resonance, although a few differences were noted (Mohammadi et al., 2005; Ornitz et al., 1996; Zhang et al., 2006). These differences probably result from the fact that our assay involved endogenous heparan sulfate on developing lenses, whereas the other systems depend on exogenous heparin. Nevertheless, our data confirm that many of the FGF-FGFR interactions require *N*-sulfated glucosamine residues in heparan sulfate, suggesting that *Ndst1* inactivation could potentially disrupt multiple FGF-FGFR-signaling pathways during eye development. Recent studies demonstrating modest. or even no, lens defects in FGFR1, FGFR2 and FGFR3 single mutants support this idea (Garcia et al., 2005; Huang et al., 2003; Zhao et al., 2006). Therefore, our study of the *Ndst1* gene provides an attractive model to unravel the complexity of FGF signaling in eye development.

The authors thank S. Conway, T. Glaser, C. Heldin, B. Hogan, G. Oliver, N. Takahashi, P. ten Dijke and Pfizer for mouse, antibodies, probes and reagents; E. Creshaw for help with immunohistochemistry; and M. Rauchman for helpful discussion. The work was supported by grants from March of Dimes Birth Defects Foundation (#5-FY05-49 to X.Z.); NIH (RO1 EY017061 to X.Z. and R37GM33063 and HL57345 to J.D.E.); and DFG (German Research Council) (GR1748/1-1 and GR1748/1-2 to K.G.).

References

Ahn, K., Mishina, Y., Hanks, M. C., Behringer, R. R. and Crenshaw, E. B., 3rd (2001). BMPR-IA signaling is required for the formation of the apical ectodermal ridge and dorsal-ventral patterning of the limb. *Development* **128**, 4449-4461.

Aikawa, J., Grobe, K., Tsujimoto, M. and Esko, J. D. (2001). Multiple isozymes of heparan sulfate/heparin GlcNAc N-deacetylase/GlcN N-sulfotransferase. Structure and activity of the fourth member, NDST4. *J. Biol. Chem.* **276**, 5876-5882.

Allen, B. L. and Rapraeger, A. C. (2003). Spatial and temporal expression of

heparan sulfate in mouse development regulates FGF and FGF receptor assembly. *J. Cell Biol.* **163**, 637-648.
Bai, X., Wei, G., Sinha, A. and Esko, J. D. (1999). Chinese hamster ovary cell mutants defective in glycosaminoglycan assembly and glucuronosyltransferase I. *J. Biol. Chem.* **274**, 13017-13024.
Belenkaya, T. Y., Han, C., Yan, D., Opoka, R. J., Khodoun, M., Liu, H. and Lin, X. (2004). Drosophila Dpp morphogen movement is independent of dynamin-mediated endocytosis but regulated by the glypican members of heparan sulfate proteoglycans. *Cell* **119**, 231-244.
Brown, N. L., Patel, S., Brzezinski, J. and Glaser, T. (2001). Math5 is required for retinal ganglion cell and optic nerve formation. *Development* **128**, 2497-2508.
Chow, R. L. and Lang, R. A. (2001). Early eye development in vertebrates. *Annu. Rev. Cell Dev. Biol.* **17**, 255-296.
Corson, L. B., Yamanaka, Y., Lai, K. M. and Rossant, J. (2003). Spatial and temporal patterns of ERK signaling during mouse embryogenesis. *Development* **130**, 4527-4537.
Dakubo, G. D., Wang, Y. P., Mazerolle, C., Campsall, K., McMahon, A. P. and Wallace, V. A. (2003). Retinal ganglion cell-derived sonic hedgehog signaling is required for optic disc and stalk neuroepithelial cell development. *Development* **130**, 2967-2980.
Darnell, D. K., Stark, M. R. and Schoenwolf, G. C. (1999). Timing and cell interactions underlying neural induction in the chick embryo. *Development* **126**, 2505-2514.
DasGupta, R. and Fuchs, E. (1999). Multiple roles for activated LEF/TCF transcription complexes during hair follicle development and differentiation. *Development* **126**, 4557-4568.
David, G., Bai, X. M., Van der Schueren, B., Cassiman, J. J. and Van den Berghe, H. (1992). Developmental changes in heparan sulfate expression: in situ detection with mAbs. *J. Cell Biol.* **119**, 961-975.
de Iongh, R. and McAvoy, J. W. (1993). Spatio-temporal distribution of acidic and basic FGF indicates a role for FGF in rat lens morphogenesis. *Dev. Dyn.* **198**, 190-202.
Dudley, A. T. and Robertson, E. J. (1997). Overlapping expression domains of bone morphogenetic protein family members potentially account for limited tissue defects in BMP7 deficient embryos. *Dev. Dyn.* **208**, 349-362.
Esko, J. D. and Selleck, S. B. (2002). Order out of chaos: assembly of ligand binding sites in heparan sulfate. *Annu. Rev. Biochem.* **71**, 435-471.
Faber, S. C., Dimanlig, P., Makarenkova, H. P., Shirke, S., Ko, K. and Lang, R. A. (2001). Fgf receptor signaling plays a role in lens induction. *Development* **128**, 4425-4438.
Faber, S. C., Robinson, M. L., Makarenkova, H. P. and Lang, R. A. (2002). Bmp signaling is required for development of primary lens fiber cells. *Development* **129**, 3727-3737.
Fan, G., Xiao, L., Cheng, L., Wang, X., Sun, B. and Hu, G. (2000). Targeted disruption of NDST-1 gene leads to pulmonary hypoplasia and neonatal respiratory distress in mice. *FEBS Lett.* **467**, 7-11.
Favata, M. F., Horiuchi, K. Y., Manos, E. J., Daulerio, A. J., Stradley, D. A., Feeser, W. S., Van Dyk, D. E., Pitts, W. J., Earl, R. A., Hobbs, F. et al. (1998). Identification of a novel inhibitor of mitogen-activated protein kinase kinase. *J. Biol. Chem.* **273**, 18623-18632.
Ford-Perriss, M., Guimond, S. E., Greferath, U., Kita, M., Grobe, K., Habuchi, H., Kimata, K., Esko, J. D., Murphy, M. and Turnbull, J. E. (2002). Variant heparan sulfates synthesized in developing mouse brain differentially regulate FGF signaling. *Glycobiology* **12**, 721-727.
Forsberg, E., Pejler, G., Ringvall, M., Lunderius, C., Tomasini-Johansson, B., Kusche-Gullberg, M., Eriksson, I., Ledin, J., Hellman, L. and Kjellen, L. (1999). Abnormal mast cells in mice deficient in a heparin-synthesizing enzyme. *Nature* **400**, 773-776.
Furukawa, T., Mukherjee, S., Bao, Z. Z., Morrow, E. M. and Cepko, C. L. (2000). rax, Hes1, and notch1 promote the formation of Muller glia by postnatal retinal progenitor cells. *Neuron* **26**, 383-394.
Furuta, Y. and Hogan, B. L. (1998). BMP4 is essential for lens induction in the mouse embryo. *Genes Dev.* **12**, 3764-3775.
Garcia, C. M., Yu, K., Zhao, H., Ashery-Padan, R., Ornitz, D. M., Robinson, M. L. and Beebe, D. C. (2005). Signaling through FGF receptor-2 is required for lens cell survival and for withdrawal from the cell cycle during lens fiber cell differentiation. *Dev. Dyn.* **233**, 516-527.
Garcia-Garcia, M. J. and Anderson, K. V. (2003). Essential role of glycosaminoglycans in Fgf signaling during mouse gastrulation. *Cell* **114**, 727-737.
Gotoh, N., Ito, M., Yamamoto, S., Yoshino, I., Song, N., Wang, Y., Lax, I., Schlessinger, J., Shibuya, M. and Lang, R. A. (2004). Tyrosine phosphorylation sites on FRS2alpha responsible for Shp2 recruitment are critical for induction of lens and retina. *Proc. Natl. Acad. Sci. USA* **101**, 17144-17149.
Govindarajan, V. and Overbeek, P. A. (2001). Secreted FGFR3, but not FGFR1, inhibits lens fiber differentiation. *Development* **128**, 1617-1627.
Grobe, K., Ledin, J., Ringvall, M., Holmborn, K., Forsberg, E., Esko, J. D. and Kjellen, L. (2002). Heparan sulfate and development: differential roles of the N-acetylglucosamine N-deacetylase/N-sulfotransferase isozymes. *Biochim. Biophys. Acta* **1573**, 209-215.
Grobe, K., Inatani, M., Pallerla, S. R., Castagnola, J., Yamaguchi, Y. and Esko, J. D. (2005). Cerebral hypoplasia and craniofacial defects in mice lacking heparan sulfate Ndst1 gene function. *Development* **132**, 3777-3786.
Haerry, T. E., Heslip, T. R., Marsh, J. L. and O'Connor, M. B. (1997). Defects in glucuronate biosynthesis disrupt Wingless signaling in Drosophila. *Development* **124**, 3055-3064.
Han, C., Belenkaya, T. Y., Khodoun, M., Tauchi, M. and Lin, X. (2004). Distinct and collaborative roles of Drosophila EXT family proteins in morphogen signalling and gradient formation. *Development* **131**, 1563-1575.
Huang, J. X., Feldmeier, M., Shui, Y. B. and Beebe, D. C. (2003). Evaluation of fibroblast growth factor signaling during lens fiber cell differentiation. *Invest. Ophthalmol. Vis. Sci.* **44**, 680-690.
Humphries, D. E., Wong, G. W., Friend, D. S., Gurish, M. F., Qiu, W. T., Huang, C., Sharpe, A. H. and Stevens, R. L. (1999). Heparin is essential for the storage of specific granule proteases in mast cells. *Nature* **400**, 769-772.
Inatani, M., Irie, F., Plump, A. S., Tessier-Lavigne, M. and Yamaguchi, Y. (2003). Mammalian brain morphogenesis and midline axon guidance require heparan sulfate. *Science* **302**, 1044-1046.
Kirkpatrick, C. A., Dimitroff, B. D., Rawson, J. M. and Selleck, S. B. (2004). Spatial regulation of Wingless morphogen distribution and signaling by Dally-like protein. *Dev. Cell* **7**, 513-523.
Kitaoka, T., Aotaki-Keen, A. E. and Hjelmeland, L. M. (1994). Distribution of FGF-5 in the rhesus macaque retina. *Invest. Ophthalmol. Vis. Sci.* **35**, 3189-3198.
Koziel, L., Kunath, M., Kelly, O. G. and Vortkamp, A. (2004). Ext1-dependent heparan sulfate regulates the range of Ihh signaling during endochondral ossification. *Dev. Cell* **6**, 801-813.
Lawson, K. A., Dunn, N. R., Roelen, B. A., Zeinstra, L. M., Davis, A. M., Wright, C. V., Korving, J. P. and Hogan, B. L. (1999). Bmp4 is required for the generation of primordial germ cells in the mouse embryo. *Genes Dev.* **13**, 424-436.
Leteux, C., Chai, W., Nagai, K., Herbert, C. G., Lawson, A. M. and Feizi, T. (2001). 10E4 antigen of Scrapie lesions contains an unusual nonsulfated heparan motif. *J. Biol. Chem.* **276**, 12539-12545.
Lin, X. (2004). Functions of heparan sulfate proteoglycans in cell signaling during development. *Development* **131**, 6009-6021.
Lin, X. and Perrimon, N. (1999). Dally cooperates with Drosophila Frizzled 2 to transduce Wingless signalling. *Nature* **400**, 281-284.
Lin, X., Buff, E. M., Perrimon, N. and Michelson, A. M. (1999). Heparan sulfate proteoglycans are essential for FGF receptor signaling during Drosophila embryonic development. *Development* **126**, 3715-3723.
Lin, X., Wei, G., Shi, Z., Dryer, L., Esko, J. D., Wells, D. E. and Matzuk, M. M. (2000). Disruption of gastrulation and heparan sulfate biosynthesis in EXT1-deficient mice. *Dev. Biol.* **224**, 299-311.
Lovicu, F. J. and Overbeek, P. A. (1998). Overlapping effects of different members of the FGF family on lens fiber differentiation in transgenic mice. *Development* **125**, 3365-3377.
Lovicu, F. J. and McAvoy, J. W. (2001). FGF-induced lens cell proliferation and differentiation is dependent on MAPK (ERK1/2) signalling. *Development* **128**, 5075-5084.
Macdonald, R., Barth, K. A., Xu, Q., Holder, N., Mikkola, I. and Wilson, S. W. (1995). Midline signalling is required for Pax gene regulation and patterning of the eyes. *Development* **121**, 3267-3278.
Martinez-Morales, J. R., Del Bene, F., Nica, G., Hammerschmidt, M., Bovolenta, P. and Wittbrodt, J. (2005). Differentiation of the vertebrate retina is coordinated by an FGF signaling center. *Dev. Cell* **8**, 565-574.
McWhirter, J. R., Goulding, M., Weiner, J. A., Chun, J. and Murre, C. (1997). A novel fibroblast growth factor gene expressed in the developing nervous system is a downstream target of the chimeric homeodomain oncoprotein E2A-Pbx1. *Development* **124**, 3221-3232.
Mohammadi, M., Olsen, S. K. and Ibrahimi, O. A. (2005). Structural basis for fibroblast growth factor receptor activation. *Cytokine Growth Factor Rev.* **16**, 107-137.
Munchberg, S. R. and Steinbeisser, H. (1999). The Xenopus Ets transcription factor XER81 is a target of the FGF signaling pathway. *Mech. Dev.* **80**, 53-65.
Nguyen, M. and Arnheiter, H. (2000). Signaling and transcriptional regulation in early mammalian eye development: a link between FGF and MITF. *Development* **127**, 3581-3591.
Norton, W. H., Ledin, J., Grandel, H. and Neumann, C. J. (2005). HSPG synthesis by zebrafish Ext2 and Extl3 is required for Fgf10 signalling during limb development. *Development* **132**, 4963-4973.
Ornitz, D. M., Xu, J., Colvin, J. S., McEwen, D. G., MacArthur, C. A., Coulier, F., Gao, G. and Goldfarb, M. (1996). Receptor specificity of the fibroblast growth factor family. *J. Biol. Chem.* **271**, 15292-15297.
Paine-Saunders, S., Viviano, B. L., Zupicich, J., Skarnes, W. C. and Saunders, S. (2000). glypican-3 controls cellular responses to Bmp4 in limb patterning and skeletal development. *Dev. Biol.* **225**, 179-187.
Pellegrini, L., Burke, D. F., von Delft, F., Mulloy, B. and Blundell, T. L. (2000).

Crystal structure of fibroblast growth factor receptor ectodomain bound to ligand and heparin. *Nature* **407**, 1029-1034.
Raible, F. and Brand, M. (2001). Tight transcriptional control of the ETS domain factors Erm and Pea3 by Fgf signaling during early zebrafish development. *Mech. Dev.* **107**, 105-117.
Rapraeger, A. C., Krufka, A. and Olwin, B. B. (1991). Requirement of heparan sulfate for bFGF-mediated fibroblast growth and myoblast differentiation. *Science* **252**, 1705-1708.
Rasmussen, J. T., Deardorff, M. A., Tan, C., Rao, M. S., Klein, P. S. and Vetter, M. L. (2001). Regulation of eye development by frizzled signaling in Xenopus. *Proc. Natl. Acad. Sci. USA* **98**, 3861-3866.
Ringvall, M., Ledin, J., Holmborn, K., van Kuppevelt, T., Ellin, F., Eriksson, I., Olofsson, A. M., Kjellen, L. and Forsberg, E. (2000). Defective heparan sulfate biosynthesis and neonatal lethality in mice lacking N-deacetylase/N-sulfotransferase-1. *J. Biol. Chem.* **275**, 25926-25930.
Robinson, M. L. and Overbeek, P. A. (1996). Differential expression of alpha A- and alpha B-crystallin during murine ocular development. *Invest. Ophthalmol. Vis. Sci.* **37**, 2276-2284.
Roehl, H. and Nusslein-Volhard, C. (2001). Zebrafish pea3 and erm are general targets of FGF8 signaling. *Curr. Biol.* **11**, 503-507.
Schlessinger, J., Plotnikov, A. N., Ibrahimi, O. A., Eliseenkova, A. V., Yeh, B. K., Yayon, A., Linhardt, R. J. and Mohammadi, M. (2000). Crystal structure of a ternary FGF-FGFR-heparin complex reveals a dual role for heparin in FGFR binding and dimerization. *Mol. Cell* **6**, 743-750.
Skaper, S. D., Kee, W. J., Facci, L., Macdonald, G., Doherty, P. and Walsh, F. S. (2000). The FGFR1 inhibitor PD 173074 selectively and potently antagonizes FGF-2 neurotrophic and neurotropic effects. *J. Neurochem.* **75**, 1520-1527.
Smith, A. N., Miller, L. A., Song, N., Taketo, M. M. and Lang, R. A. (2005). The duality of beta-catenin function: a requirement in lens morphogenesis and signaling suppression of lens fate in periocular ectoderm. *Dev. Biol.* **285**, 477-489.
Song, H. H., Shi, W., Xiang, Y. Y. and Filmus, J. (2005). The loss of glypican-3 induces alterations in Wnt signaling. *J. Biol. Chem.* **280**, 2116-2125.
Stickens, D., Zak, B. M., Rougier, N., Esko, J. D. and Werb, Z. (2005). Mice deficient in Ext2 lack heparan sulfate and develop exostoses. *Development* **132**, 5055-5068.
Stump, R. J., Ang, S., Chen, Y., von Bahr, T., Lovicu, F. J., Pinson, K., de Iongh, R. U., Yamaguchi, T. P., Sassoon, D. A. and McAvoy, J. W. (2003). A role for Wnt/beta-catenin signaling in lens epithelial differentiation. *Dev. Biol.* **259**, 48-61.
Tsang, M. and Dawid, I. B. (2004). Promotion and attenuation of FGF signaling through the Ras-MAPK pathway. *Sci. STKE* **2004**, pe17.
Tsonis, P. A., Vergara, M. N., Spence, J. R., Madhavan, M., Kramer, E. L., Call, M. K., Santiago, W. G., Vallance, J. E., Robbins, D. J. and Del Rio-Tsonis, K. (2004). A novel role of the hedgehog pathway in lens regeneration. *Dev. Biol.* **267**, 450-461.
Turnbull, J. E., Fernig, D. G., Ke, Y., Wilkinson, M. C. and Gallagher, J. T. (1992). Identification of the basic fibroblast growth factor binding sequence in fibroblast heparan sulfate. *J. Biol. Chem.* **267**, 10337-10341.
van den Born, J., Salmivirta, K., Henttinen, T., Ostman, N., Ishimaru, T., Miyaura, S., Yoshida, K. and Salmivirta, M. (2005). Novel heparan sulfate structures revealed by monoclonal antibodies. *J. Biol. Chem.* **280**, 20516-20523.
Vogel-Hopker, A., Momose, T., Rohrer, H., Yasuda, K., Ishihara, L. and Rapaport, D. H. (2000). Multiple functions of fibroblast growth factor-8 (FGF-8) in chick eye development. *Mech. Dev.* **94**, 25-36.
Wang, S. W., Kim, B. S., Ding, K., Wang, H., Sun, D., Johnson, R. L., Klein, W. H. and Gan, L. (2001). Requirement for math5 in the development of retinal ganglion cells. *Genes Dev.* **15**, 24-29.
Wawersik, S., Purcell, P., Rauchman, M., Dudley, A. T., Robertson, E. J. and Maas, R. (1999). BMP7 acts in murine lens placode development. *Dev. Biol.* **207**, 176-188.
Wigle, J. T., Chowdhury, K., Gruss, P. and Oliver, G. (1999). Prox1 function is crucial for mouse lens-fibre elongation. *Nat. Genet.* **21**, 318-322.
Yamamoto, Y., Stock, D. W. and Jeffery, W. R. (2004). Hedgehog signalling controls eye degeneration in blind cavefish. *Nature* **431**, 844-847.
Yayon, A., Klagsbrun, M., Esko, J. D., Leder, P. and Ornitz, D. M. (1991). Cell surface, heparin-like molecules are required for binding of basic fibroblast growth factor to its high affinity receptor. *Cell* **64**, 841-848.
Yuasa, J., Hirano, S., Yamagata, M. and Noda, M. (1996). Visual projection map specified by topographic expression of transcription factors in the retina. *Nature* **382**, 632-635.
Zhang, X., Friedman, A., Heaney, S., Purcell, P. and Maas, R. L. (2002). Meis homeoproteins directly regulate Pax6 during vertebrate lens morphogenesis. *Genes Dev.* **16**, 2097-2107.
Zhang, X., Heaney, S. and Maas, R. L. (2003). Cre-loxp fate-mapping of Pax6 enhancer active retinal and pancreatic progenitors. *Genesis* **35**, 22-30.
Zhang, X., Ibrahimi, O. A., Olsen, S. K., Umemori, H., Mohammadi, M. and Ornitz, D. M. (2006). Receptor specificity of the fibroblast growth factor family. The complete mammalian FGF family. *J. Biol. Chem.* **281**, 15694-15700.
Zhao, H., Yang, Y., Partanen, J., Ciruna, B. G., Rossant, J. and Robinson, M. L. (2006). Fibroblast growth factor receptor 1 (Fgfr1) is not essential for lens fiber differentiation in mice. *Mol. Vis.* **12**, 15-25.
Zhao, S., Hung, F. C., Colvin, J. S., White, A., Dai, W., Lovicu, F. J., Ornitz, D. M. and Overbeek, P. A. (2001). Patterning the optic neuroepithelium by FGF signaling and Ras activation. *Development* **128**, 5051-5060.
Zhu, C. C., Dyer, M. A., Uchikawa, M., Kondoh, H., Lagutin, O. V. and Oliver, G. (2002). Six3-mediated auto repression and eye development requires its interaction with members of the Groucho-related family of co-repressors. *Development* **129**, 2835-2849.